ISSN 2278-2540 | DOI: 10.51583/IJLTEMAS | Volume XV, Issue X, October 2026

Experimental and Numerical Investigation of the Tensile Bond Behavior of Post-Installed Reinforcing Bar in Concrete

Shina Peter Babatunde[1*], Emmanuel Eberechuku Ndububa[1], Olumide Williams Oseni[1], Wisdom Mfe Tavaku[2], Nneka Blessing Ekwe[2], Caleb A. Ogunlowo[4]

[1] Department of Civil Engineering, University of Abuja, Nigeria.

[2] Nigeria Building and Road research Institute, Road Research Department

[3] Department of Chemical Engineering, University of Abuja, Nigeria.

[4]Department of Civil Engineering, Ladoke Akintola University of Technology, Ogbomosho, Oyo State, Nigeria.

***Corresponding Author**

DOI: https://doi.org/10.51583/IJLTEMAS.2026.151000032

Received: 19 August 2026; Accepted: 24 August 2026; Published: 31 October 2026

ABSTRACT

Post-installed rebar (PIR) systems have become an essential solution for the repair, strengthening, and retrofitting of reinforced concrete structures by providing reliable anchorage without extensive structural reconstruction. However, accurately predicting their tensile behavior and failure mechanisms under varying service conditions remains challenging due to the complex interaction among the reinforcing bar, adhesive layer, and surrounding concrete. This study presents a combined experimental and three-dimensional finite element investigation of the tensile behavior of PIR systems using ABAQUS. The numerical model incorporated the Concrete Damaged Plasticity (CDP) model for concrete and an elastoplastic constitutive model for reinforcing steel to simulate nonlinear material behavior and bond degradation. Numerical simulations were conducted for embedment depths of 100, 200, and 300 mm under monotonic pull-out loading and thermal exposure. The numerical predictions were validated against experimental results and demonstrated excellent agreement, with prediction errors below 5% under monotonic loading. The results showed that increasing embedment depth significantly enhanced pull-out resistance, with pull-out loads increasing from 2.426 kN at 100mm to 28.702 kN at 200mm and 74.242 kN at 300mm for experimental and 2.510 kN at 100 mm to 29.133 kN at 200 mm and 73.510 kN at 300 mm for numerical under monotonic loading. Thermal exposure reduced bond integrity and promoted premature pull-out failure. Overall, the validated finite element model reliably predicted the structural response of PIR systems and provides an effective tool for evaluating bond behavior, optimizing anchorage design, and improving the safety, durability, and performance of reinforced concrete retrofitting systems.

Keywords: Post-installed rebars; Tensile loading; ABAQUS; Finite element analysis; Structural retrofitting; Bond behavior; Pull-out resistance.

INTRODUCTION

The increasing demand for sustainable infrastructure has heightened the need for effective methods of repairing, strengthening, and extending the service life of existing reinforced concrete structures [1]. Across the world, many buildings, bridges, and other civil engineering facilities require rehabilitation due to aging, increased service loads, changes in structural design requirements, seismic upgrading, and deterioration caused by environmental exposure. Complete demolition and reconstruction are often economically impractical and environmentally unsustainable. Consequently, structural rehabilitation techniques that improve the performance of existing structures while minimizing disruption have become an essential aspect of modern civil engineering practice [2].

ISSN 2278-2540 | DOI: 10.51583/IJLTEMAS | Volume XV, Issue X, October 2026

Among the available rehabilitation techniques, post-installed rebar (PIR) systems have gained widespread acceptance because they provide a reliable means of connecting new structural elements to existing concrete. Unlike cast-in-place reinforcement, post-installed rebars are installed after the concrete has hardened by drilling holes into the concrete and anchoring reinforcing bars using adhesive or mechanical anchorage systems. This method offers flexibility during renovation and retrofitting projects and has become widely adopted in applications such as beam and slab extensions, column jacketing, bridge rehabilitation, and seismic strengthening [3].

The structural performance of a post-installed rebar system depends largely on the effectiveness of the bond developed between the reinforcing bar, adhesive material, and surrounding concrete. When subjected to tensile loading, stresses are transferred through the adhesive layer into the concrete, making the bond interface

the most critical region governing structural behavior. The efficiency of this load transfer mechanism is influenced by several factors, including embedment depth, adhesive properties, concrete strength, bar diameter, installation quality, and loading conditions. Depending on these factors, failure may occur through adhesive debonding, pull-out failure, concrete cone breakout, concrete splitting, or yielding of the reinforcing steel. Understanding these mechanisms is essential for ensuring the safe design and long-term performance of rehabilitation systems [4].

Experimental investigations have significantly advanced the understanding of PIR behavior under tensile loading by providing valuable information on bond strength, pull-out resistance, stiffness characteristics, and failure modes. However, laboratory testing alone has several limitations. Experimental programs are often expensive, time-consuming, and constrained by the number of specimens that can be tested. Furthermore, many internal mechanisms, such as stress redistribution, crack propagation, and bond degradation within the concrete–adhesive–steel interface, cannot be directly observed during physical testing. These limitations have encouraged the increasing use of advanced numerical simulation techniques to complement experimental investigations and provide deeper insight into structural behavior [5].

Among the available computational approaches, the finite element method (FEM) has become one of the most powerful tools for analyzing reinforced concrete systems because of its ability to model complex material behavior and nonlinear structural response [6]. Commercial software such as ABAQUS enables detailed simulation of concrete cracking, steel plasticity, adhesive behavior, and contact interactions under different loading conditions. When properly calibrated and validated with experimental data, finite element models can accurately predict load–displacement behavior, stress distribution, interface debonding, and failure progression while reducing the need for extensive experimental testing. As a result, numerical modelling has become an important component of structural design, assessment, and optimization [7].

Despite considerable progress in both experimental and numerical research, accurately predicting the tensile behavior of post-installed rebar systems remains challenging. The nonlinear interaction between concrete, adhesive, and reinforcing steel involves complex bond–slip relationships, progressive cracking, stiffness degradation, and changing failure mechanisms that are difficult to capture using simplified analytical methods [8]. In addition, although embedment depth is widely recognized as one of the most influential design parameters, its effect on pull-out behavior under different loading scenarios has not been comprehensively evaluated within a unified experimental and numerical framework. This knowledge gap limits the ability of engineers to optimize anchorage design for different service conditions [9].

This study addresses these challenges by combining laboratory testing with three-dimensional finite element modelling in ABAQUS to investigate the tensile behavior of post-installed rebar systems. The numerical model was developed and validated using experimental results before being employed to evaluate the influence of embedment depth under monotonic pull-out loading and environmental exposure conditions. The study further examines force–displacement behavior, pull-out resistance, bond degradation, stiffness characteristics, and failure mechanisms to provide a comprehensive understanding of the structural response of PIR systems. By integrating experimental observations with validated numerical simulations, this research provides practical insights that can contribute to improved anchorage design, more reliable structural rehabilitation strategies, and enhanced durability of reinforced concrete structures.

ISSN 2278-2540 | DOI: 10.51583/IJLTEMAS | Volume XV, Issue X, October 2026

a b

Figure 1. Schematic illustration of the post-installed rebar (PIR) system practical site work application: (a) Installed reinforcing bar embedded in hardened concrete using adhesive anchorage; (b) Sectional view showing the concrete, adhesive layer, and reinforcing steel bar.

Source: Ahmadu Bello Wy, Central Business Dis, Abuja 900103, Federal Capital Territory, Nigeria. Bus terminal project, 2024.

METHODOLOGY

This section presents the experimental and numerical procedures adopted for investigating the tensile behavior of post-installed rebar (PIR) systems. The methodology integrates laboratory testing with finite element modeling using ABAQUS to ensure reliable validation of results.

Experimental Materials and Method

Materials

The materials used in the study are ordinary Portland limestone cement (PLC), coarse aggregates, fine aggregates, reinforcement bars, epoxy-based adhesives and water. The PLC (Dangote cement of grade 42.5r) was purchased from a local cement store, 12mm TMT reinforcement bars and epoxy-based adhesives (Epoxy Acrylate), all within Abuja FCT, Nigeria. In addition, natural river sand (4.75mm) was used as fine aggregates, and a crushed, angular, porous graded material, having a maximum aggregate size of 19mm, was used as coarse aggregate.

Test Samples

Concrete cube samples of (150x150x150) mm were prepared with a mix ratio 1:2:4 to perform a compressive strength test. Likewise, 150mm diameter and 300mm height cylindrical samples was casted and three (3) specimen were prepared for each embedded length i.e. for 100mm depth, 200mm depth and 300mm depth. After pouring the concrete, it was allowed to cure for 28days. For the study the concrete strength was 30N/mm2 and 12mm of tensile strength of 500N/mm2 were used.

Pull-out Test

The tensile bond behavior of the post-installed reinforcing bars was experimentally investigated using a 200kN capacity Universal Test Machine (UTM). The pull-out testing procedure was conducted with reference [10], which specifies the use of a tensile testing machine of adequate capacity for applying tensile force to a reinforcing steel bar anchored in a concrete block and for measuring the corresponding load and displacement. The experimental test was designed to determine the load-displacement response, ultimate pull-out load, displacement at peak load, and initial stiffness of the post-installed reinforcing bar embedded in concrete. A monotonically increasing axial tensile load was applied to the reinforcing bar using 200kN UTM, while the applied load and corresponding displacement were continuously displacement were continuously recorded until failure.

ISSN 2278-2540 | DOI: 10.51583/IJLTEMAS | Volume XV, Issue X, October 2026

Environmental Exposure to Thermal Test.

A controlled elevated-temperature exposure of **110 °C** was applied to evaluate the thermal stability of the epoxy–rebar–concrete bond system. The temperature was selected as a mild elevated condition representing a possible heat-transfer scenario during construction and repair activities. Previous studies have shown that elevated temperatures can influence the mechanical properties of adhesives used for post-installed reinforcement [11], the bond behavior of post-installed rebar connections [12]. After exposure, the specimens were cooled to ambient temperature before pullout testing to assess changes in their residual bond performance.

Test Setup and Procedure

Monotonic Pull-Out Test

The pull-out test was conducted on the cylindrical concrete samples using a 200kN Capacity UTM. C30 concrete were prepared and cured for 28days before installation of the post-installed reinforcing bars. 12mm diameter reinforcing bar was installed into pre-drilled holes at the center of the cylindrical concrete sample using the selected chemical adhesive (Epoxy Acrylate). The embedment length used were 100mm,200mm and 300mm. The drilled holes were cleaned to remove drilling dust and loose particles. The adhesive was poured into the drilled hole to the entire embedded length, Figure 2 shows reinforcing bar was installed in to the holes using the selected adhesive as binding agents. The specimens were allowed to cure for 28days full cured before testing. As seen in figure 3, a UTM was used to perform the pull-out test on the post-installed reinforcements in concrete and applied load and corresponding displacement were continuously recorded by the UTM data-acquisition system. Testing was continued until pull-out, debonding and concrete failure. The resulting load-displacement curves were used to determine the maximum pull-out load, displacement at maximum load and initial stiffness.

Figure 2. Bar Installed in Drilled Holes with Adhesive as Binding Agents

Figure 3. Post -installed Concrete Sample Fixed to Model and the applied load and corresponding displacement were continuously recorded by the UTM data-acquisition system

ISSN 2278-2540 | DOI: 10.51583/IJLTEMAS | Volume XV, Issue X, October 2026

Exposure to Thermal Pull-Out Test.

Following the procedure of monotonic pull-out test, the cylindrical concrete specimens was subjected to thermal exposure in a laboratory oven. As seen in figure 4, the specimen was placed inside the oven and heated to a target temperature of 110 °C. The oven temperature was monitored to ensure that the required temperature was condition was achieved. After the completion of the heating period, the specimen was removed from the oven and allowed to cool before pull-out test was performed. The load and displacement response recorded by UTM system was compare with that of unexposed specimens to quantify the influence of temperature on the post-installed rebar bond performance.

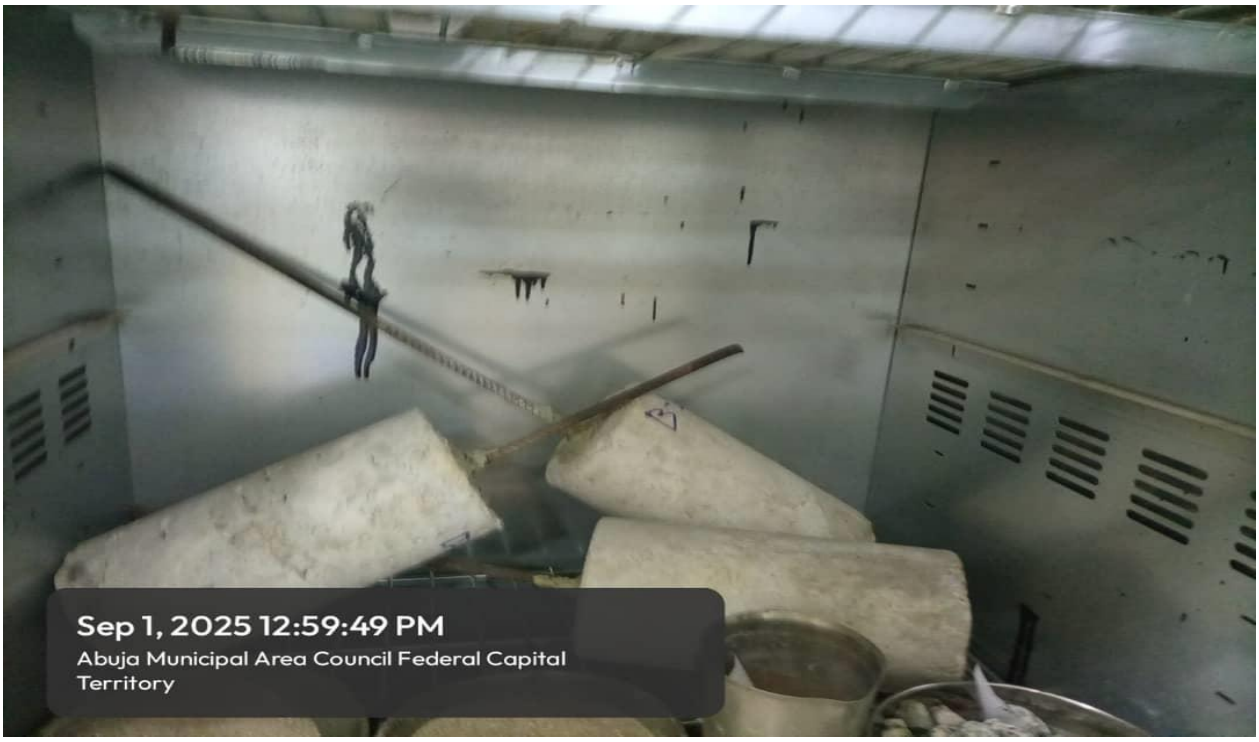

Figure 4. Post-installed Rebar in the Laboratory Oven

Failure Modes

The main failure modes of post-installed single anchor in uncracked concrete under a tension force are concrete cone failure, bar rupture failure, pull-out (bond) failure, concrete spitting failure, and pull-through failure [13], [14] & [15]. The failure mode are:

1) ***Concrete Cone Failure*** - Concrete cone failure occurs in post-installed concrete with shallow embedded depths where the capacity of concrete is low. It involves the extraction of a cone-shaped portion of the post-installed concrete, having its highest point at the embedded end of the anchor because of the circumferential stresses. Moreover, there is usually a crack at 35° from the base of the anchor, which procedure the cone caused by tensile failure.
2) **Pull-out (Bond) Failure** - It is usually caused by improper installation, such as unclean holes or partial bonding between the adhesive and concrete or adhesive and rebar. It involves debonding an anchor over its entire embedded length that can occur at the adhesive-concrete or adhesive-rebar interface.
3) **Concrete Splitting failure** – Concrete splitting failure generally occurs when the size of the concrete is small, and the anchor is installed close to the edge of the concrete mass. It can be avoided by providing minimum edge distance. Moreover, failure load is usually reduced compared to cone breakout failure.
4) **Pull-through failure** - This failure is the combination of failure at the adhesive-concrete and adhesive-rebar interfaces. It occurs in anchor extraction from a concrete mass without significant concrete failure.
5) **Bar Rupture Failure** - This failure represents the upper value of the highest load carried by an anchor, and it rarely happens except in high-strength concrete with high embedded depths and low rebar strengths. The rebar type and cross-sectional area usually define the failure.

ISSN 2278-2540 | DOI: 10.51583/IJLTEMAS | Volume XV, Issue X, October 2026

Finite Element Model Development (Numerical Procedure)

To complement the experimental investigation, a three-dimensional (3D) nonlinear finite element model of the post-installed rebar (PIR) system was developed using ABAQUS/Standard. The numerical model was designed to reproduce the pull-out test configuration and simulate the structural response of the adhesive anchorage system under tensile loading. The model comprised three principal components: the concrete substrate, reinforcing steel bar, and adhesive layer, all represented according to the dimensions of the experimental specimens.

The concrete specimen was modelled as a cylinder with dimensions corresponding to those used in the laboratory tests (100mm diameter x 300mm height), while a 12 mm diameter reinforcing steel bar was positioned concentrically within the drilled hole at the specified embedment depths of 100 mm, 200 mm, and 300 mm. The adhesive layer was explicitly incorporated into the model to simulate the transfer of stresses between the reinforcing steel and the surrounding concrete. The geometry of the assembled finite element model is presented in Figure 5,

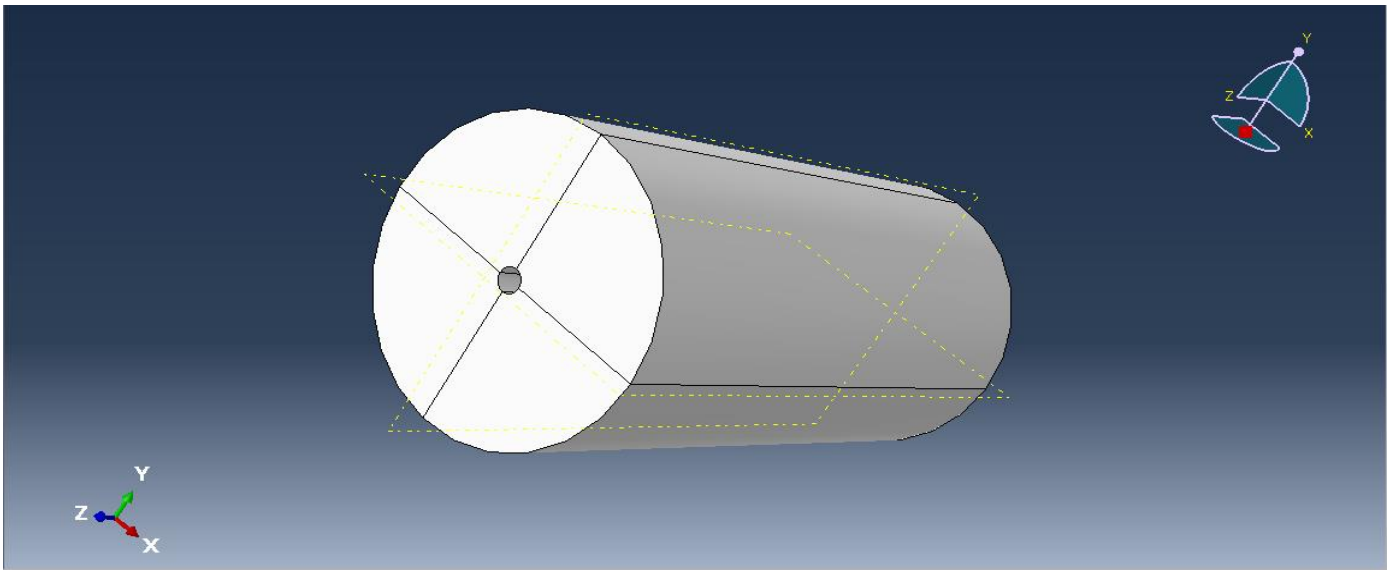

Figure 5. Modelled Cylinder Concrete Specimen in Abaqus

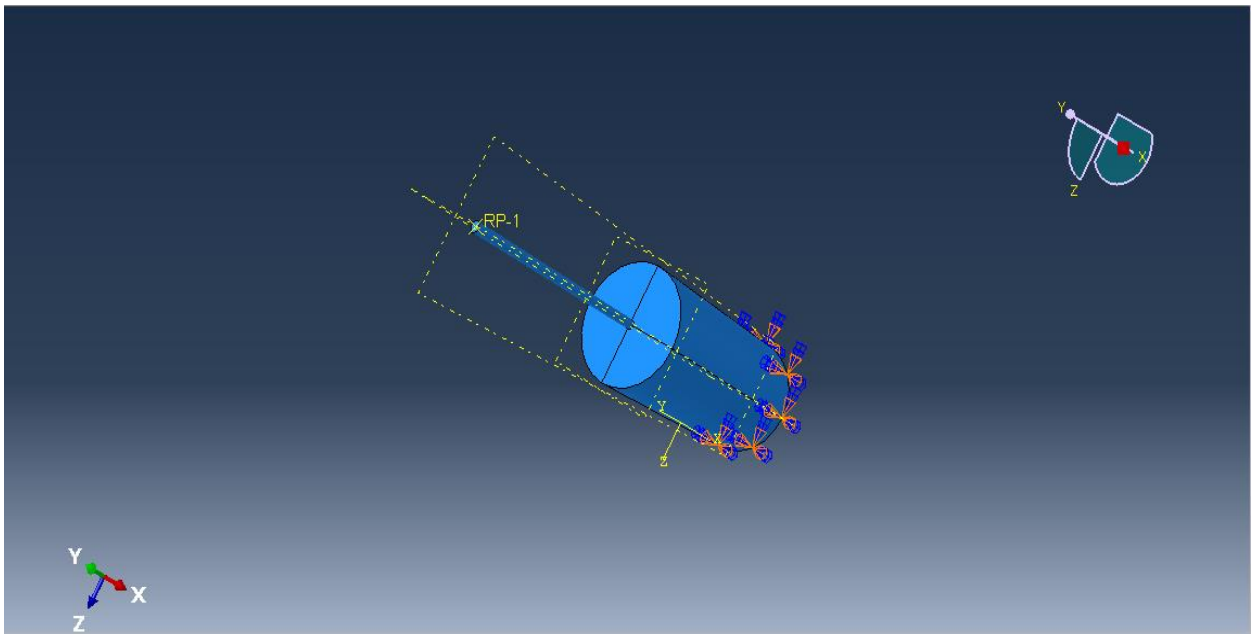

Figure 6. Three-dimensional finite element model of the post-installed rebar (PIR) system developed in ABAQUS, showing the concrete specimen, reinforcing steel bar, and reference point (RP-1) used for load

ISSN 2278-2540 | DOI: 10.51583/IJLTEMAS | Volume XV, Issue X, October 2026

application.

The numerical model was created using the Part, Property, Assembly, Step, Interaction, Load, Mesh, and Job modules available in ABAQUS. Individual parts representing the concrete, reinforcing bar, and adhesive were first created before being assembled into a single computational model. Appropriate geometric constraints were applied to ensure accurate positioning of the reinforcing bar within the concrete specimen.

To ensure consistency between the laboratory investigation and numerical simulation, the model geometry and specimen dimensions were developed directly from the experimental configuration. This approach minimized modelling uncertainties and enabled direct comparison between the numerical predictions and the experimental pull-out responses during model validation.

Material Properties and Constitutive Models

The finite element model was developed by assigning appropriate material properties and constitutive models to the concrete, reinforcing steel, and adhesive layer to accurately simulate the mechanical behavior of the post-installed rebar (PIR) system under tensile loading. The selected material models were chosen based on their ability to reproduce the nonlinear response of the constituent materials observed during experimental testing.

Concrete

Concrete was modelled using the Concrete Damaged Plasticity (CDP) model available in ABAQUS. The CDP model was selected because it provides a realistic representation of concrete behavior under both compressive and tensile loading by accounting for plastic deformation, tensile cracking, compressive crushing, and progressive stiffness degradation. The elastic properties of the concrete, including Young's modulus, Poisson's ratio, and density, were first defined before introducing the nonlinear compressive and tensile stress–strain relationships. Damage parameters for both compression and tension were specified to simulate crack initiation, propagation, and material degradation throughout the pull-out analysis.

Reinforcing Steel

The reinforcing steel bar was modelled as an elastic–plastic material with isotropic strain hardening. The material was assumed to behave linearly within the elastic range before yielding and subsequently exhibited plastic deformation according to the defined hardening behavior.

The elastic modulus, Poisson's ratio, yield strength, and density of the reinforcing steel were assigned based on the material properties used in the experimental programmed. This constitutive model enabled realistic prediction of stress development and deformation of the reinforcing bar during pull-out loading.

Adhesive Material

The adhesive was modelled as the bonding medium responsible for transferring tensile forces from the reinforcing steel to the surrounding concrete. It was assumed to exhibit linear elastic behaviour within the applied loading range and was assigned appropriate mechanical properties, including Young's modulus, Poisson's ratio, and density.

The adhesive layer played a significant role in maintaining bond integrity and facilitating stress transfer across the concrete–steel interface throughout the numerical simulation.

2.5 Boundary Conditions and Loading

To accurately replicate the experimental pull-out test, appropriate boundary conditions and loading configurations were applied to the finite element model. The boundary conditions were established to prevent rigid body motion while ensuring that the numerical simulation closely represented the laboratory testing arrangement. The bottom surface of the concrete block was fully restrained by fixing all translational degrees

ISSN 2278-2540 | DOI: 10.51583/IJLTEMAS | Volume XV, Issue X, October 2026

of freedom (Ux = Uy = Uz = 0), thereby preventing displacement in the three principal directions throughout the analysis. This constraint ensured that the applied tensile load was transferred through the post-installed rebar system without introducing unintended movement of the concrete specimen.

A displacement-controlled axial tensile load was applied to the free end of the reinforcing steel bar through a reference point (RP-1) using a coupling constraint. The prescribed displacement ranged from 0 to 100mm depending on the loading scenario considered, enabling the complete pull-out response of the anchorage system to be captured under monotonic loading conditions.

The analysis was performed using the Static, General analysis procedure available in ABAQUS/Standard. The load was applied incrementally to facilitate convergence during nonlinear analysis and to accurately capture the initiation and progression of concrete cracking, bond degradation, and stress redistribution within the adhesive anchorage system. The displacement-controlled loading approach provided stable numerical solutions and enabled direct comparison between the numerical predictions and the corresponding experimental pull-out test results. The adopted boundary conditions and loading strategy ensured realistic simulation of the structural behavior of the post-installed rebar system and provided a reliable basis for evaluating the effects of embedment depth, and thermal exposure on pull-out performance.

Model Interaction and Mesh Generation

To accurately simulate the interaction between the constituent materials, surface-to-surface contact interactions were defined between the reinforcing steel, adhesive layer, and surrounding concrete. A penalty contact formulation was employed to represent the bond behavior at the interfaces, allowing stress transfer while accommodating limited relative slip during loading. This approach enabled realistic simulation of bond degradation, interface debonding, and stress redistribution as the applied tensile load increased.

The finite element model was discretized using an appropriate meshing strategy to achieve an optimal balance between computational efficiency and solution accuracy. The concrete cylinder, reinforcing steel bar, and adhesive layer were meshed using eight-node linear brick reduced integration (C3D8R) solid, and tetrahedral (C3DR) elements available in ABAQUS. These elements were selected because of their ability to accurately simulate nonlinear material behavior while minimizing computational cost. A non-uniform mesh was adopted throughout the model. A finer mesh density was applied around the concrete–adhesive–rebar interface, where high stress concentrations, bond-slip behavior, and damage initiation were expected. Conversely, a relatively coarser mesh was used in regions away from the interface to reduce computational time without significantly affecting the accuracy of the numerical results. A typical meshed model is presented in Figure 7.

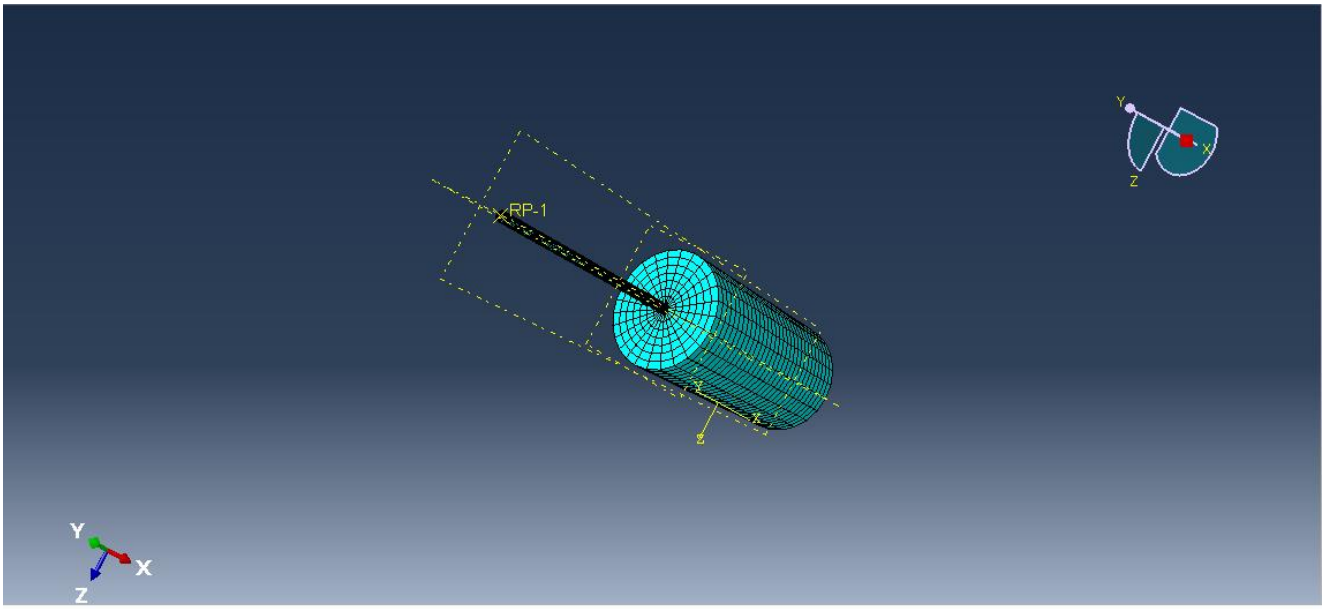

Figure 7. Finite element mesh of a post-installed rebar (PIR) model developed in ABAQUS.

ISSN 2278-2540 | DOI: 10.51583/IJLTEMAS | Volume XV, Issue X, October 2026

The adopted mesh refinement and contact interaction strategy ensured numerical stability and improved the prediction of the load–displacement response, stress distribution, and failure mechanisms of the post-installed rebar system under pull-out scenarios.

EXPERIMENTAL AND NUMERICAL (ABAQUS) RESULTS AND DISCUSSION

Experimental Data

Concrete (C25/C30):

- Elastic Modulus (Ei) = 30,000 MPa
- Poisson's ratio (v) = 0.20
- Concrete Strength (Fi) = 30 MPa
- Tensile of Concrete (Ft) = 3.3 MPa
- Compression Strain = 0.0020
- Tension Strain = 0.00012

Steel (12mm):

- Yield Strength (Fy) = 500MPa
- Ultimate strength (Fu) = 600 MPa
- Elastic Modulus (Es) = 200 GPa
- Poisson's ratio = 0.30
- Plastic stress-strain curve = 0.022

Acrylate Epoxy Data

- Adhesive elastic Modulus = 3.13 GN/m^2
- Adhesive tensile Strength = 13 N/mm^2
- Adhesive shear strength = 14 N/mm^2 (Mpa)
- Fraction energy = 24 N/mm
- Density = 1700 Kg/m^3

Experimental and Numerical Result on Monotonic Pull-out Loading

Experimental Result on Monotonic Loading

Table 1: Experimental result for monotonic pull-out loading of average value of three specimen test in each embedment length.

Loading Condition	Embedment Depth (mm)	Peak Force (kN)	Displacement at Peak (mm)
	100	2.426	1.087
Monotonic Pull-out Loading	200	28.702	8.344
	300	74.242	41.695

Table 1, shown the experimental results of pull-out behavior on embedment length. The pull-out capacity increased from 2.426 kN at 100 mm to 28.702 kN at 200 mm and 74.242 kN at 300 mm. Correspondingly, the displacement at peak load increased from 1.087 mm to 8.344 mm and 41.695 mm, respectively.

ISSN 2278-2540 | DOI: 10.51583/IJLTEMAS | Volume XV, Issue X, October 2026

Numerical (ABAQUS) Results

Table 2: Abaqus result for monotonic pull-out loading

Loading Condition	**Embedment Depth (mm)**	**Peak Force (kN)**	**Displacement at Peak (mm)**
	100	2.51	0.749
Monotonic Pull-out Loading	200	29.133	8.102
	300	73.51	40.5

Table 2, presents the numerical results for monotonic pull-out loading at embedment depths of 100mm,200mm and 300mm, showing peak forces of 2.510 kN, 29.133 kN, and 73.510 kN, respectively, peak displacement increased correspondingly from 0.749 mm,8.102 mm and to 40.500 mm, indicating that greater embedment depth enhances bond stress distribution, delays debonding, and increases pull-out nonlinearly.

Table 3. Monotonic pull-out loading Numerical– Experimental Comparison

Embedment length	Experimental peak load(kN)	Abaqus peak load (kN)	Peak-load error (%)	Experimental displacement at peak (mm)	Abaqus displacement at peak (mm)	Displacement error (%)	Experimental initial stiffness (kN/mm)	Abaqus initial stiffness (kN/mm)	Stiffness error (%)
100 mm	2.426	2.51	3.46	1.087	0.749	31.09	2.27	6	164.32
200 mm	28.702	29.133	1.5	8.344	8.102	2.9	4.84	6.15	27.07
300 mm	74.242	73.51	3.18	41.695	40.5	2.18	7.19	6.9	4.03
Overall	—	—	MAPE = 2.71	—	—	MAPE= 12.06	—	—	MAPE=65.14

Table 3, shown comparing the experimental and Abaqus results in terms of peak pull-out capacity, displacement at peak load and initial stiffness for the three embedment lengths. The predicted peak loads were 2.510, 29.133 and 73.510 kN for the 100, 200mm and 300mm embedment lengths, respectively, compared with experimental values of 2.426, 28.702 and 74.242 kN. The corresponding percentage errors were 3.46%, 1.50% and 0.99%, respectively. For displacement at peak load, the numerical predictions were 0.749, 8.102 and 40.500 mm, compared with experimental values of 1.087, 8.344 and 41.695 mm, resulting in errors of 31.09%, 2.90% and 2.87%, respectively. The relatively large discrepancy at 100 mm indicates that the model does not reproduce the deformation response of the shortest embedment length as accurately as the longer embedment lengths. The initial stiffness values predicted by Abaqus were 6.00, 6.15 and 6.90 kN/mm for the 100, 200 and 300mm specimens, respectively, compared with experimental values of 2.27, 4.84 and 7.19 kN/mm. The corresponding errors were 164.32%, 27.07% and 4.03%. The relatively large stiffness discrepancy at the shorter embedment lengths may be associated with the sensitivity of the initial load–

ISSN 2278-2540 | DOI: 10.51583/IJLTEMAS | Volume XV, Issue X, October 2026

displacement response to local bond stiffness, interface properties, installation effects and the selection of the linear region used to determine experimental stiffness.

Experimental and Numerical Result on Thermal-Exposure @ 110 °C Pull-Out Loading

Loading Condition	**Embedment Depth (mm)**	**Peak Force (kN)**	**Displacement at Peak (mm)**	**Stiffness at Peak (kN/mm)**
Thermal-Exposure at 110 °C Pull-out Loading	100mm	5.915	29.562	1.153
	200mm	22.189	6.869	1.003
	300mm	27.161	17.957	1.121

Table 4. Experimental pull-out behavior after thermal exposure

Table 5. Numerical pull-out behavior after thermal exposure

Loading Condition	**Embedment Depth (mm)**	**Peak Force (kN)**	**Displacement at Peak (mm)**	**Stiffness at Peak (kN/mm)**
Thermal-Exposure at 110 °C Pull-out Loading	100mm	7.096	6.217	0.871
	200mm	22.619	13.64	1.265
	300mm	27.054	10.8	1.91

Table 6. Thermal-exposure pull-out loading Numerical– Experimental Comparison

Embedment length	Experimental peak load (kN)	Abaqus peak load (kN)	Peak-load error (%)	Experimental displacement at peak (mm)	Abaqus displacement at peak (mm)	Displacement error (%)	Experimental initial stiffness (kN/mm)	Abaqus initial stiffness (kN/mm)	Stiffness error (%)
100 mm	5.915	7.096	19.97	29.562	6.217	78.97	1.153	0.871	24.49
200 mm	22.189	22.619	1.94	6.869	13.64	98.58	1.003	1.265	26.09
300 mm	27.161	27.054	0.4	17.957	10.8	39.68	1.121	1.91	70.35
Overall	—	—	MAPE = 7.43	—	—	MAPE= 72.47	—	—	MAPE=40.32

Tables 4,5 and 7 shown the experimental and numerical pull-out responses following exposure to 110 °C. The

ISSN 2278-2540 | DOI: 10.51583/IJLTEMAS | Volume XV, Issue X, October 2026

experimental peak pull-out force increased from 5.915 kN at 100 mm embedment to 22.189 kN and 27.161 kN at 200 and 300 mm, respectively. The corresponding numerical predictions were 7.096, 22.619, and 27.054 kN. The numerical model therefore reproduced the peak pull-out capacity with errors of 19.97%, 1.94%, and 0.39%, respectively. The experimental stiffness values were 1.153, 1.003, and 1.121 kN/mm, compared with 0.871, 1.265, and 1.910 kN/mm from the numerical model. The results indicate good agreement in peak pull-out capacity at the 200 and 300 mm embedment depths, although greater differences are observed in the stiffness and displacement responses, particularly for the 100 mm specimen. The deviated in displacement and stiffness, indicating that model may not fully capture bond degradation after thermal exposure. The thermal-exposure numerical model produced a MAPE of 7.43% for peak pull-out load, indicating good agreement with the experimental results. The corresponding MAPE values for displacement at peak load and initial stiffness were 72.47% and 40.32%, respectively. The relatively higher errors in displacement and stiffness indicate that the model reproduced the ultimate pull-out capacity more accurately than the deformation and stiffness response.

Influence of Embedment Depth on Pull-Out Behavior

The numerical results demonstrate that embedment depth is the primary parameter governing the pull-out performance of the post-installed rebar (PIR) system. As summarized in Table 1 and illustrated in Figures 8–10, the ultimate pull-out capacity increased markedly with increasing embedment depth under monotonic loading. The specimen with a 100 mm embedment depth developed a peak pull-out load of 2.510 kN, whereas the 200 mm and 300 mm specimens achieved peak loads of 29.133 kN and 73.510 kN, respectively. This substantial increase in load-carrying capacity indicates that extending the embedment length significantly improves the anchorage performance of the PIR system as indicate by [16]

The observed behavior can be attributed to the larger bonded surface area available for stress transfer between the reinforcing steel, adhesive layer, and surrounding concrete. At shallow embedment depths, the limited contact area concentrates bond stresses over a relatively short anchorage length, promoting premature adhesive debonding and reducing the load that can be transferred before failure. This behavior is evident in

the 100 mm specimen, where adhesive failure occurred before significant bond mobilization could be achieved. As the embedment depth increased to 200 mm and 300 mm, the bonded interface became sufficiently long to distribute stresses more uniformly along the anchorage length [17]. Consequently, mechanical interlock between the deformed reinforcing bar and the adhesive-concrete interface became progressively mobilized, allowing the system to sustain substantially higher tensile loads before failure.

This behavior suggests that increasing embedment length not only improves the ultimate pull-out resistance but also delays the progression of localized bond damage by engaging a larger proportion of the bonded interface [18].

The predicted failure modes also evolved with embedment depth. The shallow embedment specimen failed predominantly through adhesive debonding, whereas the deeper embedment specimens exhibited concrete splitting failure. This transition indicates that once adequate bond strength is developed along the adhesive interface, the surrounding concrete becomes the controlling component of the anchorage system. Rather than interface failure governing the response, tensile stresses generated within the concrete eventually exceed its fracture capacity, resulting in splitting failure. Such behavior is characteristic of well-developed bonded anchorage systems in which the interface strength exceeds the tensile resistance of the surrounding concrete [16].

These findings agree with previous investigations that identified embedment depth as one of the most influential parameters affecting the tensile performance of adhesive-anchored reinforcement systems. Longer embedment lengths provide improved bond development, more efficient stress transfer, and greater anchorage efficiency, ultimately resulting in higher pull-out capacities and enhanced structural reliability. The present results therefore confirm that adequate embedment depth is essential for maximizing the load-transfer mechanism and ensuring stable structural performance of post-installed rebar systems under tensile loading [19].

ISSN 2278-2540 | DOI: 10.51583/IJLTEMAS | Volume XV, Issue X, October 2026

Effect of Thermal Exposure on Bond Performance

The thermal exposure analysis demonstrated a considerable reduction in the pull-out performance of the post-installed rebar (PIR) system across all embedment depths. As presented in Table 4&5, pull-out loads under thermal exposure conditions were consistently lower than those obtained under monotonic loading. Although the pull-out capacity increased with embedment depth, from 5.915 kN at 100 mm to 22.189 kN at 200 mm and 27.161 kN at 300 mm for experimental, and 7.096 kN at 100mm to 22.619 kN at 200mm and 27.054 kN at 300mm for Numerical, the improvement was substantially smaller than that observed under normal loading conditions. This indicates that thermal exposure adversely affected the efficiency of the bond mechanism regardless of the embedment length [20].

The reduction in structural performance can be attributed to deterioration of the adhesive interface and weakening of the surrounding concrete matrix. In the numerical model, thermal exposure was simulated by reducing the stiffness properties of the interface and concrete surface layers before the pull-out analysis. This degradation reduced the ability of the adhesive layer to effectively transfer tensile stresses from the reinforcing steel into the surrounding concrete, thereby limiting the development of full bond strength. As a result, the load–displacement responses exhibited lower stiffness and earlier failure compared with the corresponding monotonic loading responses [21].

These findings agree with previous investigations reporting that environmental actions such as elevated temperature, progressively reduce adhesive strength and bond integrity in post-installed anchorage systems. Such deterioration accelerates interface debonding, reduces frictional resistance, and limits stress transfer across the bonded region. The present results therefore demonstrate that thermal exposure can significantly compromise the structural performance of adhesive-anchored reinforcement, even when adequate embedment depth is provided. Consequently, durability considerations should be incorporated into the design and assessment of post-installed rebar systems intended for service in aggressive environmental conditions to ensure long-term structural safety and reliability [22].

CONCLUSIONS AND RECOMMENDATIONS

This study presented a combined numerical and experimental investigation of post-installed rebar (PIR) systems subjected to tensile loading, with emphasis on the influence of embedment depth, pull-out loading and thermal exposure. A validated three-dimensional finite element model was developed using ABAQUS to simulate load–displacement behavior and bond interaction. The following conclusions are made based on the result of this study:

1. Embedment depth is a major determinant of PIR performance: The pull-out capacity increased with embedment length under pull-out loading, showing that longer bonded lengths provide improved load transfer and greater resistance to failure.

2. Thermal exposure weakened the anchorage response: The results indicate that long-term thermal exposure conditions can reduce the effectiveness of the bond interface and lower the pull-out resistance of the system.

3. Pull-out loading: The Abaqus model shown good agreement with experimental load, particularly at 200 and 300mm

4. The finite element approach remains suitable for PIR studies: The result patterns obtained are consistent with the expected behavior of bonded reinforcement systems and support the use of numerical modeling for evaluating PIR performance under different service conditions.

Several recommendations are made for future research based on the research findings. These are:

1. Investigating different adhesive materials to determine their performance under thermal exposure loading.

ISSN 2278-2540 | DOI: 10.51583/IJLTEMAS | Volume XV, Issue X, October 2026

2. Studying other load types such as shear, fatigue, and combined loading for a more complete understanding of PIR behavior and Including full-scale experimental validation to strengthen the reliability of the numerical findings.

3. Extending the study to include more embedment lengths and rebar diameters in order to develop a broader design database.

4. For critical retrofit works, pull-out verification should be carried out before field application

ACKNOWLEDGEMENTS

The authors acknowledge the contribution of the Department of Civil Engineering at the University of Abuja and Nigeria and Nigeria Building and Road research Institute, Road Research Department (NBRRI), towards the conduct of this research.

Ethical approval: Not applicable

Conflict of interest: The authors declare that there are no conflicts of interests.

Funding: The study has not received any external funding

Data availability: All data associated with this study are presented in the paper

REFERENCES

1. Looi, D. T., Lee, Y. F., Su, R. K., & Zhang, Y. (2020). Design and installation of post-installed reinforcements: A state-of-the-art review. *HKIE Transactions*, *27*(2).
2. Zakian, P., & Kaveh, A. (2023). Seismic design optimization of engineering structures: a comprehensive review. *Acta Mechanica*, *234*(4), 1305-1330.
3. Bolboli, S. (2024). Rounding the corner of construction by implementing circular economy: developing a process model for construction using reused materials and enhancing it with advanced technologies.
4. Haidar, H. H., Mussa, F. I., Dawood, A. O., Ghazi, A. A., & Gabbar, R. A. (2020). Experimental study of post installed rebar anchor systems for concrete structure. *Civil and Environmental Engineering*, *16*(2), 308-319.
5. Chen, Z. (2023). Non-concrete breakout failure modes of concrete mechanical anchors in tension-a literature review. *Construction and Building Materials*, *366*, 130222.
6. Pir, İ., Tufekci, M., Acarer Arat, S., & Tufekci, E. (2026). Mechanics of Epoxy Nanocomposites: A Study on the Synergy of the Reinforcements. *ACS omega*, *11*(8), 13379-13404.
7. Abdollahi-Mamoudan, F., Ibarra-Castanedo, C., & Maldague, X. P. (2025). Non-destructive testing and evaluation of hybrid and advanced structures: a comprehensive review of methods, applications, and emerging trends. *Sensors*, *25*(12), 3635.
8. Saleh, B. (2025). Numerical Evaluation of Corrosion-Induced Degradation in Reinforced Concrete Beams Using Finite Element Analysis in ABAQUS.
9. He, W., Wang, C., Wang, S., Yao, L., Wu, J., & Xie, D. (2020). Tensile mechanical behavior and failure mechanisms of multihole fiber metal laminates—Experimental characterization and numerical prediction. *Journal of Reinforced Plastics and Composites*, *39*(13-14), 499-519.
10. EN 1881;2006: Products and systems for the protection and repair of concrete structures-Test methods -Testing of the anchoring products by the pull-out method.
11. Deng, et al. (2023). Influence of cure time, temperature, and moisture on mechanical properties of a fast cure adhesive for post-installed rebar application. *Construction and Building Materials, 407, 133615.*
12. Muciaccia, G., Navarrete, D.D., Pinoteau, N. & Mege, R. (2019). Effects of different test apparati and heating procedures on the bond properties of post-installed rebar connections under elevated temperatures. *Materials and Structures, 52, 47.*

ISSN 2278-2540 | DOI: 10.51583/IJLTEMAS | Volume XV, Issue X, October 2026

13. Chicchi, R., Seo, J., Varma, A.H., and Bradt, T. (2017), "Consideration of breakout failure modes in design of attachments to concrete structures", *Proceedings of the 24th Conference on Structural Mechanics in Reactor Technology*, BEXCO, Busan, Korea, August, pp.2787-2792.
14. Robson, M.N., Al-Mansouri, O., Pinoteau, N., Abate, M., McBride, K., Piccinin, R., Rémond, S., and Hoxha, D. (2022), "Experimental investigation of the concrete cone failure of bonded anchors at room and high temperature", *Applied Sciences, Vol.12, pp.4760, available at: https://doi.org/10.3390/app12094760*
15. Rao, G.A., and Arora, J. (2013), "Strength and modes of failure of adhesive anchors in confined concrete under direct tensile loading", *Proceedings of the 8th International Conference on Fracture Mechanics of Concrete and Concrete Structures*, Toledo, Spain, March, available at: https://bit.ly/FraMCoS-8-p565-pdf
16. Hu, Z., Shah, Y. I., & Yao, P. (2021). Experimental and numerical study on interface bond strength and anchorage performance of steel bars within prefabricated concrete. *Materials*, *14*(13), 3713.
17. Zhao, X., Sun, K., Huang, Q., Xu, W., Qiu, W., Ma, S., & Tang, L. (2022). Research on the reasonable anchorage length and failure characteristics of resin anchorage system. *Construction and Building Materials*, *356*, 129309.
18. Gao, J., Zhao, G., & Zhang, X. (2022). Load Transfer Mechanism and Bond–Slip Behavior of Recycled Concrete-Encased Steel (RCES) Subjected to Cyclic Loading. *Coatings*, *12*(12), 1806.
19. Boumakis, I., Marcon, M., Ninčević, K., Czernuschka, L. M., & Wan-Wendner, R. (2018). Concrete creep and shrinkage effect in adhesive anchors subjected to sustained loads. *Engineering Structures*, *175*, 790-805.
20. Perera, U. N. D., Chandrathilaka, E. R. K., Arachchi, K. K., & Gamage, J. C. P. H. (2023). Thermal sensitivity of CFRP/Steel bond exposed to prolonged water ingress. *Case Studies in Construction Materials*, *18*, e02071.
21. Hu, J., Jin, J., Xuan, S., Mi, S., Tian, W., & Liao, W. (2022). Influence of cyclical hygrothermal aging on mechanical response and structural durability of composite bolted interference-fit joints. *Thin-Walled Structures*, *173*, 108997.
22. Neupane, C. C., Lee, J., Pokharel, T., Tsang, H. H., & Gad, E. (2025). Development and challenges in finite element modelling of post-installed anchors in concrete. *Structure and Infrastructure Engineering*, *21*(2), 319-340.